

Luis Elcoro,^{a*} Olivier Pérez,^b
J. M. Perez-Mato^a and Václav
Petříček^c

^aDpto de Física de la Materia Condensada, Facultad de Ciencia y Tecnología, University of the Basque Country UPV EHU, Apdo. 644, Bilbao 48080, Spain, ^bCRISMAT, UMR CNRS 6508, 6 Bd du Maréchal Juin 14050, CEDEX 4, Caen, France, and ^cInstitute of Physics, Academy of Sciences of the Czech Republic v.v.i., Na Slovance 2, 182 21 Praha 8, Czech Republic

Correspondence e-mail: luis.elcoro@ehu.es

Unified (3 + 1)-dimensional superspace description of the 2212-type stair-like $[\text{Bi}_2\text{Sr}_3\text{Fe}_2\text{O}_9]_m[\text{Bi}_4\text{Sr}_6\text{Fe}_2\text{O}_{16}]$ family of compounds

The (3 + 1)-dimensional superspace approach is applied to describe and refine a series of sheared compounds related to layered high T_c superconducting oxides. Two commensurate members ($m = 4, 5$) of the 2212 stair-like $[\text{Bi}_2\text{Sr}_3\text{Fe}_2\text{O}_9]_m[\text{Bi}_4\text{Sr}_6\text{Fe}_2\text{O}_{16}]$ family of compounds, previously studied using single-crystal diffraction data, are analyzed. A common average unit cell has been identified and a composition-dependent modulation wavevector is proposed. The model is built using only three independent atomic domains, one for the metal atoms and two for the O atoms. The three Sr, Bi and Fe species are described using close-connected crenel-like functions forming a continuous atomic domain along the internal space. The two oxygen domains are represented by crenel functions and the displacive modulation functions are built up by Legendre polynomials recently implemented in the program *JANA2006*. Surprisingly, the results of the refinements show a striking similarity of the displacive modulations for the two compounds analyzed, indicating that a unique model can be used to describe the correlations between the atomic displacements of the 2212 stair-like series. This final model is then applied to *predict* the structure of new members of the family.

Received 17 January 2012

Accepted 23 April 2012

B-IncStrDB Reference:
6372EFFECT1

1. Introduction

The wave of superconductivity rushing into the scientific world in the middle of the eighties led to the discovery of numerous original oxides in solid state chemistry. Among them, the layered materials resulting from the intergrowth of m AMO_3 perovskite-type slabs and one block of n $\text{A}'\text{O}$ rocksalt-type slices can be highlighted; they belong to the $\text{A}'\text{-A-M-O}$ systems with $\text{A} = \text{Tl, Pb, Hg, Bi}$; $\text{A}' = \text{Sr, Ca, Ba}$ and $\text{M} = \text{Cu, Fe, Mn, Co}$. The complex formulation $\text{A}'_{n-1}\text{Sr}_2\text{A}_{m-1}\text{M}_m\text{O}_{2m+n+1}$ is commonly replaced by the simplified notation $\text{A}'-(n-1)2(m-1)m$ identifying the considered stacking. In these families of oxides, Bi-based phases are observed only for $n = 3$ implying the formation of double $[\text{BiO}]_\infty$ - $[\text{BiO}]_\infty$ layers. These phases are characterized by strong incommensurate modulations and non-stoichiometric proportions of oxygen, both displacive and occupational modulations being involved. The driving force of these two phenomena takes place in the double $[\text{BiO}]_\infty$ - $[\text{BiO}]_\infty$ layers specific for this series of oxides. Although the main effect of these modulations is to relax the mismatch between perovskite and rocksalt layers, they also offer the ability to the double $[\text{BiO}]_\infty$ - $[\text{BiO}]_\infty$ layers to periodically host an additional O atom leading to the non-stoichiometry. Consequently, the aperiodicity plays an important role in the mechanisms stabilizing these regular intergrowths. However, other possibilities for building these types of complex stacking between

perovskite and rocksalt layers have been observed; they imply more or less complicated shearing mechanisms from $A'(n-1)2(m-1)m$ parent structures. High-resolution electron microscopy (HREM) has shown numerous phases corresponding to such a stabilizing process: $\text{Bi}_{15}\text{Ba}_7\text{Sr}_7\text{Cu}_6\text{O}_{42.5}$ (Hervieu, Michel *et al.*, 1993), $\text{Bi}_6\text{Ba}_4\text{Cu}_2\text{O}_{15}$ (Hervieu, Michel *et al.*, 1993), $\text{Bi}_{16}\text{Sr}_{28}\text{Cu}_{17}\text{O}_{69}$ (Hervieu *et al.*, 1995a), $\text{Bi}_{13}\text{Ba}_2\text{Sr}_{25}\text{Fe}_{13}\text{O}_{66}$ (Hervieu *et al.*, 1995b) and $\text{Bi}_2\text{Sr}_2\text{CuO}_6$ (Darriet *et al.*, 1993). In all these phases fragments of the layers observed in the parent structures are still involved; thus segments of the double $[\text{BiO}]_{\infty}$ – $[\text{BiO}]_{\infty}$ layers subsist. Due to the shearing mechanism occurring in the stacking direction, the different layers are interrupted and connected to layers of different natures. In that way, the width of the stair-like $[\text{BiO}]_{\infty}$ – $[\text{BiO}]_{\infty}$ double segments has a strong dependence on the nominal composition in the phases mentioned. The HREM images observed suggested a *stair* or *terrace*-like stacking of successive layers indicating some kind of ordering and the *terrace* term was then adopted (Allix *et al.*, 2004). Fig. 1 shows the (a, c) projection of the $m = 5$ member of the Bi-2212 stair-like family of compounds (Allix *et al.*, 2004). This internal ordering beyond the three-dimensional standard space group assigned to the different phases also suggests the possibility of using the superspace framework to describe the structures in a more efficient way.

Although initially developed for the analysis of incommensurately modulated structures, the superspace framework

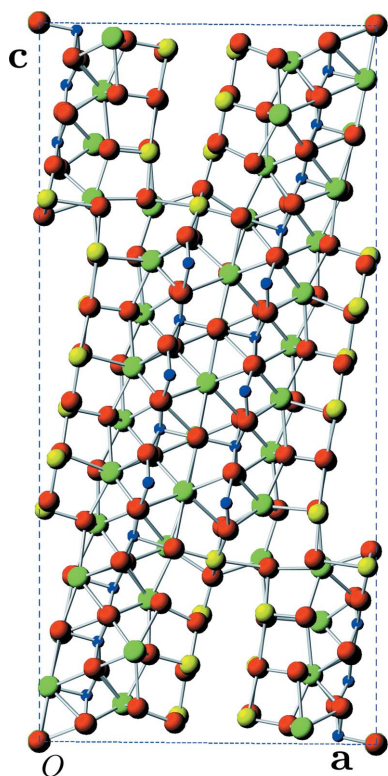


Figure 1
(a, c) projection of the $m = 5$ member of the Bi-2212 terrace-like family of compounds. Yellow, green, blue and red colors represent Bi, Sr, Fe and O atoms, respectively. This figure is in colour in the electronic version of this paper.

(de Wolff, 1974; Janner & Janssen, 1980a,b) has been revealed as a very powerful and efficient mathematical tool in the description of commensurate systems with large unit cells (Janssen *et al.*, 1992, 2007; van Smaalen, 2007). Examples of commensurate compounds with large unit cells are the series of layered compounds that can be interpreted through the stacking of a small number of different types of layers. The number and sequence of layers depends on the composition (Perez-Mato *et al.*, 1999; Elcoro *et al.*, 2000). In these systems it is possible to describe the whole structure as a deformation of a simple average structure with a smaller unit cell (average unit cell) that defines an average lattice. The existence of this underlying subperiodicity is the key point for the suitability of the superspace approach. The atomic positions that are referred to different cells of the average lattice are correlated, and the existence of these correlations can hardly be used as helpful information in a structure refinement using a standard three-dimensional approach. In the superspace formalism, these correlations are naturally included through modulations (displacive and/or occupational) superimposed to an idealized three-dimensional model with *smaller* periodicity. Other examples of a successful application of the superspace formalism to commensurate structures with large cells are the high-pressure phases Ga^{II} (Perez-Mato *et al.*, 2006), and Cs^{III} and Rb^{III} (Perez-Mato *et al.*, 2007). In these systems the subperiodicity occurs inside a two-dimensional layer. The structures can be viewed as the stacking of a small number of symmetry-related layers and, inside each layer, the atomic positions in the unit cell are correlated in such a way that it is possible to define a smaller unit cell (21 times smaller for Cs^{III}), being the atomic positions very close to the nodes of the two-dimensional average lattice. Finally, there are also families of structures that can be interpreted as the alternate stacking of two kinds of thick blocks (subsystems) whose size depends on the particular composition. The two different blocks are related by a symmetry operation (Elcoro *et al.*, 2008; Pérez *et al.*, 2012) or can be relatively shifted one with respect to the other (Michiue *et al.*, 2006).

The stair-like phases form families of compounds that can be classified by their parent structures and the involved shearing mechanisms; they exhibit strong structural analogies as the existence of comparable atomic layers but with variable lengths. However, no simple rules are shown relating the composition and the cell parameters or the symmetry of the different members. Moreover, although exhibiting classical periodicity, the existence of pseudo-symmetry, the relatively large cell parameters, the weakness of some reflections in the data sets as well as the difficulty to grow single crystals make the structure solution of these phases complex. Very often, only HREM observations are available. The accurate modelling of these structures will be an efficient tool to analyze powder diffraction data or HREM pictures. The specificity of the reciprocal space observed for these stair-like phases with the alternation of large bands of pseudo-extinct and intense reflections evokes the pattern of a modulated structure; this intensity distribution usually suggests the existence of subperiodicity. This subperiodicity is the starting point of our

superspace description of these families of compounds. However, the application of the superspace formalism to this family can be considered a limiting case of high complexity. The ratio between the volumes of the supercell and average unit cell is large even for the first members of the family (40 and 47 for the published $m = 4$ and $m = 5$ phases). The relatively few atomic domains in the superspace unit cell contain information about a large number of independent atoms of different species in the three-dimensional description (up to 24 Sr, Fe and Bi atoms in the $m = 5$ phase). Thus, some atomic domains are divided into smaller and connected step-like domains, but whose displacive modulations are described by a unique function for each coordinate. Large (and unusual) numbers of harmonics are necessary to efficiently describe these atomic domains but, even so, the superspace description has significant advantages with respect to the standard three-dimensional approach. As in other systems investigated under the superspace framework, the compounds analyzed have a unique superspace group, unique average unit cell, composition-dependent modulation wavevector and atomic domains whose size is also determined by the composition. However, a very specific feature in this case is that the displacive modulations are basically the same for phases with different composition. This strong invariance of the displacive domains with the composition had been observed in some composite structures (Thompson *et al.*, 1990; Schmid & Withers, 1994; Schmid *et al.*, 1996), but not in commensurately modulated structures and certainly not when the atomic domains are described by such a large set of Fourier terms. Probably, this is one of the best examples of families of compounds where the statement that *the superspace model is unique* can be taken literally. The facts that the modulations are described with a very large number of harmonics and that satellites are considered up to very high order are somewhat beyond the usual paradigms of the superspace framework for commensurate structures.

The paper is organized as follows: in the next section the stair-like phases are described, focusing on the two previously identified members and solved using single-crystal X-ray diffraction data, $\text{Bi}_{12}\text{Sr}_{18}\text{Fe}_{10}\text{O}_{52}$ (Hervieu *et al.*, 1997; Pérez *et al.*, 1997) and $\text{Bi}_{14}\text{Sr}_{21}\text{Fe}_{12}\text{O}_{61}$ (Allix *et al.*, 2004). In §3 the general $(3 + 1)$ -dimensional superspace construction for the whole family of compounds is introduced, including the determination of the unique superspace group, the composition-dependent modulation wavevector and the structural parameters. Subsequently, the general model is applied in the structure refinement of the two known phases. Finally, as a conclusion, based on the obtained results, realistic predictions of the structures of new members of the family are obtained.

2. Stair-like phases

The structure of the 2212-type stair-like phases can be seen as a distortion of the Bi-2212 structure with the composition $\text{Bi}_2\text{Sr}_3\text{Fe}_2\text{O}_9$ (Hervieu *et al.*, 1988), whose **(a, c)** projection is shown in Fig. 2. Large white circles (Bi), gray dots (Sr) and black dots (Fe) represent the positions of the metal atoms and

the small circles represent the O atoms. The Bi-2212 structure is related to the $(n = 3, m = 2)$ member of the large $\text{Bi}_{n-1}\text{A}_2\text{A}_{m-1}\text{M}_m\text{O}_{2m+n+1}$ series ($A = \text{Sr}, \text{Ca}, \dots$ and $M = \text{Cu}, \text{Fe}, \text{Co}, \text{Mn}$) which can also be interpreted as the intergrowth between triple rock salt-type and double perovskite-type layers. The sequence of the layers, perpendicular to the c direction, can be denoted as $([\text{SrO}]_\infty[\text{FeO}_2]_\infty[\text{SrO}]_\infty[\text{BiO}]_\infty[\text{BiO}]_\infty[\text{SrO}]_\infty[\text{FeO}_2]_\infty)_2$ in a single period along c (see Fig. 2). The collapsed or stair-like phases are obtained from the Bi-2212 structure by a distortion mechanism which consists of a double shearing process: a first shear parallel to the stacking direction every four octahedra and a second shear associated with a gliding along the a axis. At present, the structures of only two of these stair-like structures have been determined in the Bi–Sr–Fe–O system with the general formula $[\text{Bi}_2\text{Sr}_3\text{Fe}_2\text{O}_9]_m[\text{Bi}_4\text{Sr}_6\text{Fe}_2\text{O}_{16}]$, namely the $m = 4$ and $m = 5$ members with the compositions $\text{Bi}_{12}\text{Sr}_{18}\text{Fe}_{10}\text{O}_{52}$ (Pérez *et al.*, 1997) and $\text{Bi}_{14}\text{Sr}_{21}\text{Fe}_{12}\text{O}_{61}$ (Allix *et al.*, 2004), respectively. Fig. 3 shows the **(a, c)** projection of the refined structures. It can be clearly seen that the positions of the metal atoms follow in both compounds, to a first approximation, a straight line with almost equispaced atoms along the $[307]$ direction. Along this line, successive metal atoms have different y coordinates with alternate $y \sim 0$ and $y \sim \frac{1}{2}$ values. Also considering the O atoms, the whole structure can be seen as made of $[\text{SrO}]$, $[\text{BiO}]$ and $[\text{FeO}_2]$ -like columns parallel to the b direction (perpendicular to the projection of Fig. 3). The stacking of columns along the $[307]$ direction forms infinite layers where the number and sequence of columns depend on the composition. For the two known phases ($m = 4, 5$), the sequence can be expressed as $([\text{BiO}]_{m+2}[\text{SrO}]_{3(m+2)}[\text{BiO}]_{m+2}[\text{FeO}_2]_{2m+2}[\text{O}_2]_2)$ in a single

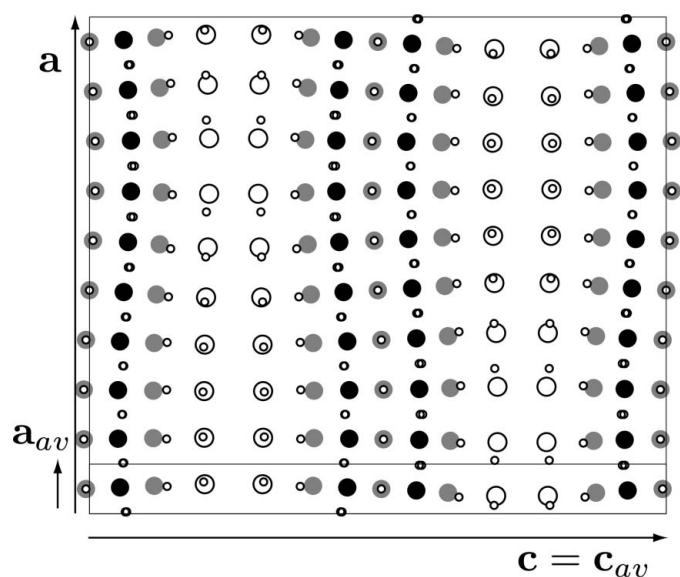


Figure 2

(a, c) projection of the Bi-2212 structure (Hervieu *et al.*, 1988) that can be considered a commensurate modulated structure. Large white circles (Bi), gray dots (Sr) and black dots (Fe) represent the positions of the metal atoms and the small circles represent the O atoms. **a** and **c** are the unit-cell vectors of the structure and $\mathbf{a}_{av} = \mathbf{a}/10$ and $\mathbf{c}_{av} = \mathbf{c}$ the unit-cell vectors of the average structure.

period in the [307] direction. Finally, the whole structure can be interpreted as the stacking of these layers with a relative shift $\mathbf{a} + 2\mathbf{c}$ between successive layers. Viewed along the b direction, the structures have a stair-like (or *terrace-like*) atomic distribution (see Fig. 3) that is due to the relative shift of the layers.

3. (3 + 1)-dimensional superspace model for the stair-like phases

The determination of the superspace model consists of several steps: first the average structure is determined. Then we deduce the primary modulation wavevector as a function of the composition. As will be explained in the following subsections, in this case it is not easy to choose the most convenient wavevector. Being commensurate structures, the diffraction patterns can be indexed using different primary wavevectors. Usually (Darriet *et al.*, 2002; Elcoro *et al.*, 2004; Izaola *et al.*, 2007; Michiue *et al.*, 2006), the best choice is the one that minimizes the number of atomic domains in the unit

cell of the superspace. However, in our case this selection gives no good results, as will be explained in the following subsections, and an alternative modulation wavevector is considered. In the following we will explain the choice of modulation wave and the resulting ideal model or reference structure. Finally, the set of independent atomic domains is also determined.

3.1. Determination of the average structure

The determination of the average lattice based on the intensities of the diffraction pattern (see Fig. 4) is not a trivial problem. The existence of sets of fringes of strong satellites limits the possible reasonable choices of the basis vectors. However, in our case the previously refined structures are, obviously, very helpful to make the best choice. As explained in the previous sections, the structure can be viewed as the alternate stacking of almost equispaced [SrO], [BiO] and [FeO₂] units along the [307] direction. The existence of equispaced units inside the unit cell along a given direction

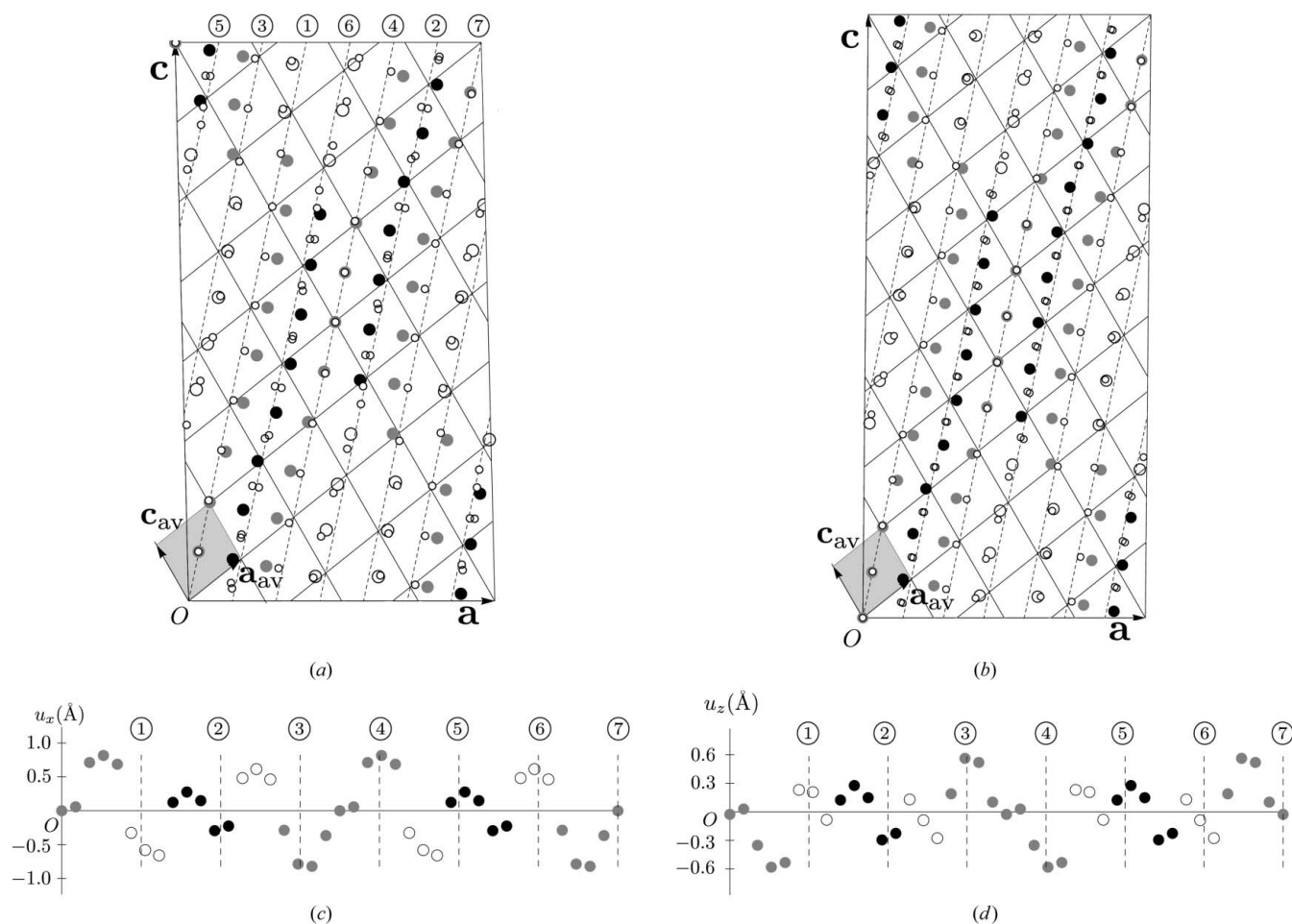


Figure 3 (a, c) projection of the (a) $m = 4$ (Pérez *et al.*, 1997) and (b) $m = 5$ (Allix *et al.*, 2004) members of the $[\text{Bi}_2\text{Sr}_3\text{Fe}_2\text{O}_9]_m[\text{Bi}_4\text{Sr}_6\text{Fe}_2\text{O}_{16}]_m$ compound family. The average lattice has been outlined. Dashed lines along the [307] direction help to show the sequence of metal-atom positions and its correlations. For the $m = 4$ compound, (c) and (d) show the components along \mathbf{a}_{av} and \mathbf{c}_{av} , respectively, of the displacements of the metal atoms at $y \sim 0$ with respect to their ideal position, *i.e.* the nodes of the average lattice in (a). The metal atoms are ordered according to their sequence along the [307] direction. Circled numbers in (c) and (d) correspond to circled positions (or equivalent positions by a supercell translation) in (a). Color labels as in Fig. 2.

indicates the existence of subperiodicity. Therefore, the stair-like structure can be interpreted as a distortion of an idealized structure with a smaller unit cell in the (\mathbf{a}, \mathbf{c}) plane. The unit cell of this basic or reference structure are the shaded cells in Fig. 3. The corresponding lattices have also been indicated. The relation between the vector basis of the supercells (\mathbf{a}, \mathbf{c}) and the vector basis of the reference structures is

$$\begin{aligned} \mathbf{a}_{\text{av}} &= \frac{m+3}{7m+12}\mathbf{a} + \frac{3}{7m+12}\mathbf{c} \\ \mathbf{b}_{\text{av}} &= \mathbf{b} \\ \mathbf{c}_{\text{av}} &= -\frac{m}{7m+12}\mathbf{a} + \frac{4}{7m+12}\mathbf{c}. \end{aligned} \quad (1)$$

The reference or basic structures correspond to idealized structures where all the metal atoms are located at the origin (atoms with $y = 0$ coordinate) or at the body center (atoms with $y = \frac{1}{2}$) of their unit cells, with only one metal atom at each value of the y coordinate ($y \sim 0, \frac{1}{2}$) in the unit cell. The O atoms in the [SrO] and [BiO] groups are shifted $\mathbf{b}/2$ with respect to the metal atom. The O atoms of the [FeO₂] groups are shifted $\pm(\mathbf{a}_{\text{av}} \pm \mathbf{b}_{\text{av}} + \mathbf{c}_{\text{av}})/4$ with respect to the Fe atom. The real structure can be considered a (commensurately) modulated structure, with the modulation being both displacive and occupational. Three different metal atoms, Sr, Bi and Fe, occupy the same average positions in the average unit cell (the origin and the body center), so they should be described by step-like functions (crenel functions) taking 0 and 1 values. When the occupation function takes the value 1 for one of the metal atoms, the other two functions representing the other

two metal atoms must take the 0 value. The O atoms occupy the same position in both the [SrO] and [BiO] groups (shifted $\mathbf{b}/2$ with respect to the corresponding metal atom), and this position is empty in the [FeO₂] unit. Therefore, there must be a step-like atomic domain representing O atoms that takes the value 1 in the regions of internal space where the atomic domain representing the Sr atom takes the value 1, and also takes the value 1 where the atomic domain of Bi takes the value 1, and takes the value 0 where the atomic domain of Fe takes the value 1. Finally, there must be two step-like atomic domains representing O atoms that take the value 1 in the regions of internal space where the atomic domain representing the Fe atom takes the value 1 and are empty otherwise. The specific set of atomic domains defining the superspace model (number and sizes of the atomic domains) depends on the chosen modulation wavevector.

3.2. Determination of the modulation wavevector

Once the average unit cell has been determined, we must determine the modulation wavevector to make the superspace construction. In this case, an appropriate choice of modulation wavevector from the diffraction pattern is not a trivial task. Fig. 4 shows schematically the $(h0\ell)$ section of the diffraction pattern of the $m = 5$ compound. The $(\mathbf{a}^*, \mathbf{c}^*)$ basis vectors of the reciprocal lattice and the $(\mathbf{a}_{\text{av}}^*, \mathbf{c}_{\text{av}}^*)$ basis vectors of the reciprocal lattice of the average structure have been indicated. There are fringes of reflections with high intensity and regions where the intensity is very small.

In principle, one should determine the primary modulation wavevector from the diffraction pattern, trying to index all reflections in the most efficient way. Usually, this means assigning indexes of increasing order to satellites with decreasing intensity. However, this rule is not always fulfilled when the superspace model contains strong modulations, as is the case when step-like atomic domains are used (see, for example, Elcoro *et al.*, 2008). This fact makes it difficult to choose the appropriate modulation wavevector. At first sight, the most natural choice could be to select $\mathbf{a}^* - \mathbf{c}^*$ as the modulation wavevector. In Fig. 4 the dashed line on the left is parallel to $\mathbf{a}^* - \mathbf{c}^*$. The line crosses alternate regions of satellites with high and low intensities so that those satellites with high intensity are indexed by low and high indices, and satellites with low intensity are indexed with intermediate indices. A more reasonable choice should keep the lowest indices for the strongest satellites. This can be done choosing a modulation wavevector almost parallel to the fringes of reflections. In Fig. 4 the dashed line on the right is almost parallel to the fringes of strong satellites, and it lies between the commensurate $3\mathbf{a}^* - \mathbf{c}^*$ and $2\mathbf{a}^* - \mathbf{c}^*$ directions. We could thus try to index the strongest satellites using a limited number of possible modulation wavevectors whose direction lies between the two given limits. However, in our case, as the three-dimensional structures for some compounds are known, we can determine the modulation wavevector in an alternative way. The superspace model is efficient if the atomic positions of different atoms result in continuous and smooth functions

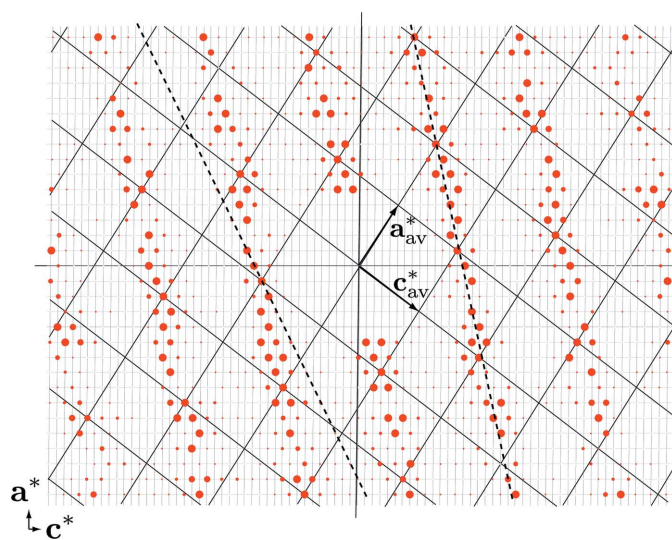


Figure 4
[010] zone axis of the diffraction pattern of the $m = 5$ member of the $[\text{Bi}_2\text{Sr}_3\text{Fe}_2\text{O}_9]_m[\text{Bi}_4\text{Sr}_6\text{Fe}_2\text{O}_{16}]$ compound family. \mathbf{a}^* and \mathbf{c}^* are the reciprocal vectors of the supercell and \mathbf{a}_{av}^* and \mathbf{c}_{av}^* are the reciprocal vectors of the average unit-cell vectors. Equation (2) gives the relation between the two sets of vectors. The solid lines show the lattices generated by the two sets of basis vectors. The dashed line on the left is parallel to $\mathbf{a}^* - \mathbf{c}^*$ and the dashed line on the right shows the direction of the fringes of strong satellites. This direction lies between the directions given by $\mathbf{q}_w = 3\mathbf{a}^* - \mathbf{c}^*$ and $\mathbf{q} = 2\mathbf{a}^* - \mathbf{c}^*$.

when they are translated into the $(3 + 1)$ -dimensional superspace description (embedding). Moreover, it is desirable to have a small number of atomic domains in the unit cell, because this means that each atomic domain represents a large number of atoms, minimizing the number of parameters to describe the whole set of atomic domains and pointing out the correlations between the positions of the atoms. In our case, it is possible to translate all the Sr, Bi, Fe and O atomic positions of the average structure (without modulations) into 2, 2, 4 and 4 atomic domains in the superspace, respectively. However, the resulting model does not agree with the known three-dimensional models, even though it is interesting first to analyze this incorrect model and then to modify it to obtain the correct one. The basis vectors of the reciprocal lattice of the average lattice are

$$\begin{aligned} \mathbf{a}_{\text{av}}^* &= 4\mathbf{a}^* + m\mathbf{c}^* \\ \mathbf{b}_{\text{av}}^* &= \mathbf{b}^* \\ \mathbf{c}_{\text{av}}^* &= -3\mathbf{a}^* + (m + 3)\mathbf{c}^* \end{aligned} \quad (2)$$

and the commensurate modulation wavevector should have the form

$$\mathbf{q} = \frac{n_1}{7m + 12} \mathbf{a}_{\text{av}}^* + \frac{n_2}{7m + 12} \mathbf{c}_{\text{av}}^* \quad (3)$$

with n_1 and n_2 integers if we want to obtain the correct unit cell of the superstructure when the three-dimensional section is considered. By inspection of Fig. 3, and taking into account the positions of the metal atoms of the same element along the lines $[307]$ and shown in the figures, it is possible to minimize the number of atomic domains taking the following as the modulation wavevector

$$\mathbf{q}_w = 3\mathbf{a}^* - \mathbf{c}^* = \frac{3(m + 2)}{7m + 12} \mathbf{a}_{\text{av}}^* - \frac{4 + 3m}{7m + 12} \mathbf{c}_{\text{av}}^*, \quad (4)$$

where subscript *w* stands for the *wrong* wavevector. Note that this vector is almost parallel to the dashed line on the right of Fig. 4. Fig. 5 shows the result of the embedding of the ideal structure into the superspace unit cell for the $m = 5$ compound using the modulation wavevector given in equation (4). These figures show just the atomic domains with the average position $(0, 0, 0)$ for Sr, Bi and Fe atoms, and $(0, \frac{1}{2}, 0)$ and $(\frac{1}{4}, \frac{1}{4}, \frac{1}{4})$ positions for the O atoms. There are also equivalent point distributions (not shown in the figure for clarity) shifted $(\frac{1}{2}, \frac{1}{2}, \frac{1}{2})$ with respect to all the points included in the figure, and extra points representing O atoms shifted $(0, \frac{1}{2}, 0)$ and $(\frac{1}{2}, 0, \frac{1}{2})$ with respect to the O atomic domain at $(\frac{1}{4}, \frac{1}{4}, \frac{1}{4})$. The superspace group of this preliminary model, *i.e.* the set of $(3 + 1)$ -dimensional symmetry operations that keeps the atomic domain distribution invariant, is $I2/m(\alpha, 0, \gamma)$ with $\alpha = \frac{3(m+2)}{7m+12}$ and $\gamma = -\frac{4+3m}{7m+12}$ (equivalent to superspace group 12.1 in Janssen *et al.*, 1992, or 12.1.4.1 in Stokes *et al.*, 2011).

This model has some drawbacks. The possible three-dimensional space groups obtained when the three-dimensional section is considered are $B2/m$, $B2_1/m$ and Bm in the supercell shown in Fig. 3 for m even [note: these space groups are equivalent to the standard $P2/m$, $P2_1/m$ and Pm space groups taking \mathbf{a} and $(\mathbf{a} + \mathbf{c})/2$ as the basis vectors of the

supercell]. For m odd the possible space groups of the three-dimensional structure are $I2/m$ or Im . They do not agree with the reported space groups $P2_1/n$ for $m = 4$ (Pérez *et al.*, 1997) and $I2$ for $m = 5$ (Allix *et al.*, 2004). In the first case, one of the possible space groups of our first tentative model is $B2/m$. The possibility of using the $B2/m$ space group in the standard three-dimensional refinement of the $m = 4$ phase has already been highlighted by the authors in their original work (Pérez *et al.*, 1997). In the first steps of the analysis by these authors, when only the positions of the metal atoms were determined, the atoms were located at special positions with $y = \pm \frac{1}{4}$. Therefore, in their first tentative model these planes were considered mirror planes and the $B2/m$ space group was assigned to the structure. However, among other problems, the Bi atoms presented large displacement parameters along the $[010]$ direction. The necessity of relaxation of the y component of the Bi atomic positions forced the authors to remove the mirror plane reducing the symmetry from $B2/m$ to $P2_1/n$. The refinement of the structure was very sensitive to

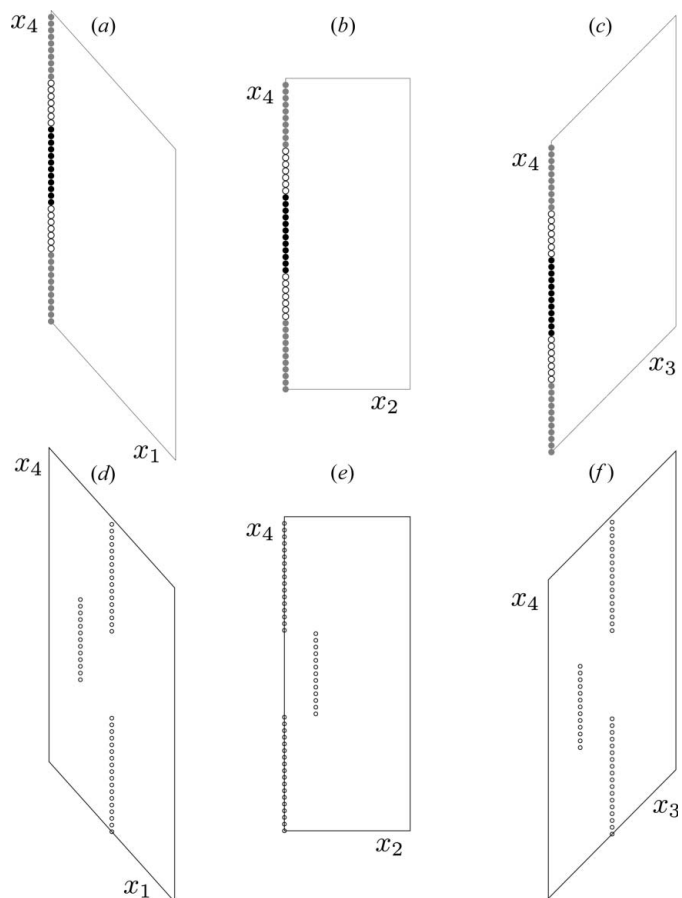


Figure 5 Atomic positions of the ideal average structure for the $m = 5$ compound, embedded into the superspace unit cell using the *wrong* modulation wavevector given by equation (4). Color labels are as in Fig. 2. The (a) (x_1, x_4) , (b) (x_2, x_4) and (c) (x_3, x_4) projections of the positions of the metal atoms have been separated from the corresponding projections (d), (e) and (f) of the positions of the O atoms for clarity. A *single* atomic domain representing the metal atoms can be clearly distinguished at the origin, and two separate O atomic domains.

Table 1

(a) Operations defining the superspace group employed in the superspace description of the 2212-type stair-like family $\text{Bi}_{4z}\text{Sr}_{6z}\text{Fe}_{1-10z}\text{O}_{4z+1}$, $X2/m(\alpha 0 \gamma)0s$ with $\alpha = \frac{1}{2} - 3z$, $\gamma = -4z$ and $z = m + 2/2(7m + 12)$, and (b) three-dimensional space groups of commensurate $m = r/s$ structures for different parities of r and s , and different choices of the real space section t .

Space groups in bold are *non-problematic* cases (see the text).

(a)			
(x_1, x_2, x_3, x_4)		$(x_1 + \frac{1}{2}, x_2 + \frac{1}{2}, x_3 + \frac{1}{2}, x_4 + \frac{1}{2})$	
$(\frac{1}{2} + x_1, \frac{1}{2} - x_2, \frac{1}{2} + x_3, x_4)$		$(x_1, -x_2, x_3, \frac{1}{2} + x_4)$	
$(-x_1, -x_2, -x_3, -x_4)$		$(\frac{1}{2} - x_1, \frac{1}{2} - x_2, \frac{1}{2} - x_3, \frac{1}{2} - x_4)$	
$(\frac{1}{2} - x_1, \frac{1}{2} + x_2, \frac{1}{2} - x_3, -x_4)$		$(-x_1, x_2, -x_3, \frac{1}{2} - x_4)$	
(b)			
$r = \text{even}$	$t = \frac{i}{2(7r+12s)}$	$t = \frac{i+1/2}{2(7r+12s)}$	$t = \text{arbitrary}$
$s = \text{odd}$	$P2/n$	$P2_1/n$	Pn
$r = \text{odd}$	$t = \frac{i}{2(7r+12s)}$	$t = \frac{i+1/2}{2(7r+12s)}$	$t = \text{arbitrary}$
$s = \text{odd}$	$I\bar{1}$	$I2$	I
$r = \text{odd}$	$t = \frac{i}{2(7r+12s)}$	$t = \frac{i+1/2}{2(7r+12s)}$	$t = \text{arbitrary}$
$s = \text{even}$	$P2_1/a$	$P2/a$	Pa

the y component of some of the Bi atoms that, in the final model, took values that correspond to displacements as large as 0.16 Å with respect to the mirror plane.

Our primary superspace model is thus compatible with the primary starting model used by Pérez *et al.* (1997). The point symmetry of the average atomic positions representing the Bi atoms does not allow any displacive modulation of the y component of the Bi atomic domain. Therefore, when the three-dimensional section is considered (for all values of t), all the Bi atoms are located at the $y = \pm \frac{1}{4}$ planes. The same anomalies arise in the analysis of the $m = 5$ phase (Allix *et al.*, 2004), where a first tentative model with the space group $I2/m$ was considered. This space group is compatible with one of the space groups given above. In Allix *et al.* (2004) the model was improved removing the m plane that restricted the y component of all the metal atoms to take the values $y = 0, \frac{1}{2}$. The above superspace model thus has to be modified. One possibility is to maintain both the average unit cell and the modulation wavevector, and to consider as a superspace group of the structure a subgroup of the given $I2/m(\alpha, 0, \gamma)$ superspace group with the same wavevector. The number of atomic domains in the unit cell remains unchanged, but the point group of the atomic domains is reduced and/or the number of independent atomic domains is larger. However, in our case there is no subgroup compatible with the reported three-dimensional space groups. This means that the average unit cell and/or the modulation wavevector must be changed.

In our second attempt, we consider a different modulation wavevector keeping the average structure. The \mathbf{q}_w modulation wavevector given by equation (4) was chosen to minimize the number of atomic domains in the superspace unit cell, which is always desirable in a superspace model. It is clear that we have to *relax* this condition and consider an alternative modulation wavevector but at the same time keeping the number of atomic domains as small as possible. It is possible to double the number of atomic domains doubling the unit cell along the

internal space or, the equivalent, considering the following as the primary modulation wavevector

$$\mathbf{q} = 2\mathbf{a}^* - \mathbf{c}^* = \frac{1}{2}(\mathbf{a}_{av}^* - \mathbf{c}_{av}^* - \mathbf{q}_w) = \left(\frac{1}{2} - 3z\right)\mathbf{a}_{av}^* - 4z\mathbf{c}_{av}^*, \quad (5)$$

where we have defined the composition-dependent parameter $z = \frac{m+2}{2(7m+12)}$ to simplify the expressions in the rest of the paper. Using this parameter, the composition can be expressed alternatively as $\text{Bi}_{4z}\text{Sr}_{6z}\text{Fe}_{1-10z}\text{O}_{4z+1}$. The limits of the z parameter are $z = 1/12$ for the $\text{Bi}_4\text{Sr}_6\text{Fe}_2\text{O}_{16}$ phase ($m = 0$) and $z = 1/14$ that corresponds to the $\text{Bi}_2\text{Sr}_3\text{Fe}_2\text{O}_9$ phase ($m = \infty$ limit). Note that the modulation wavevector in equation (5) is almost parallel to the direction given by the dashed line on the right of Fig. 4. The embedding of the reference or ideal structure into the superspace unit cell using

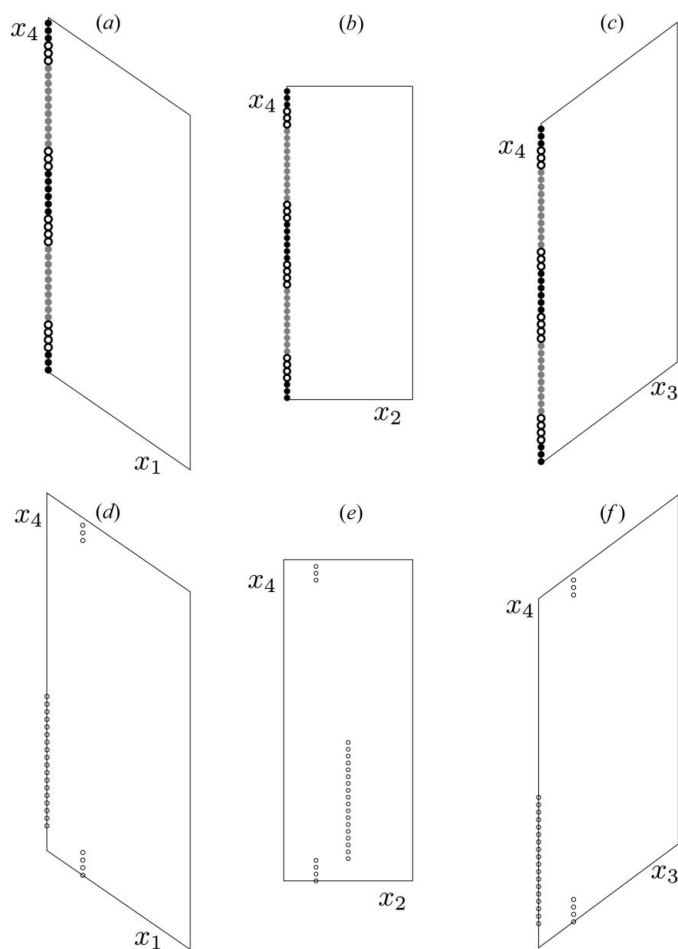


Figure 6 Atomic positions of the ideal average structure for the $m = 5$ compound, embedded into the superspace unit cell using the *good* modulation wavevector given by equation (5). This is the starting ideal model used for the structure refinements in the superspace. Color labels are as in Fig. 2. The (a) (x_1, x_4) , (b) (x_2, x_4) and (c) (x_3, x_4) projections of the positions of the metal atoms have been separated from the corresponding projections (d), (e) and (f) of the positions of the O atoms for clarity. A single atomic domain representing the metal atoms can be clearly distinguished at the origin, and two separate O atomic domains.

Table 2

Modulation wavevector and relationship between the basis vectors of the average structure and of the superstructure for all rational ($m = r/s$) compositions both in direct and reciprocal spaces.

To simplify some expressions, the composition-dependent parameter $z = m + 2/2(7m + 12)$ has been used.

Chemical formula	$\text{Bi}_{4z}\text{Sr}_{6z}\text{Fe}_{1-10z}\text{O}_{4z+1}$	
Superspace group	$X\frac{2}{m}(\alpha 0 \gamma)0s$	$X = (\frac{1}{2}, \frac{1}{2}, \frac{1}{2}, \frac{1}{2})$
Modulation wavevector	$\mathbf{q} = \underbrace{(\frac{1}{2} - 3z)}_{\alpha} \mathbf{a}_{\text{av}}^* + \underbrace{-4z}_{\gamma} \mathbf{c}_{\text{av}}^*$	
Average cell	$a_{\text{av}} \simeq 3.59 \text{ \AA}$ $b_{\text{av}} \simeq 5.49 \text{ \AA}$ $c_{\text{av}} \simeq 3.46 \text{ \AA}$	$\beta_{\text{av}} \simeq 81.90^\circ$
Transformation in direct space	$\mathbf{a}_{\text{av}} = (9z - \frac{1}{2})\mathbf{a} + \frac{1}{s}(21z - \frac{3}{2})\mathbf{c}$ $\mathbf{b}_{\text{av}} = \mathbf{b}$ $\mathbf{c}_{\text{av}} = (12z - 1)\mathbf{a} + \frac{1}{s}(28z - 2)\mathbf{c}$	$\mathbf{a} = 4\mathbf{a}_{\text{av}} - 3\mathbf{c}_{\text{av}}$ $\mathbf{b} = \mathbf{b}_{\text{av}}$ $\mathbf{c} = r\mathbf{a}_{\text{av}} + (r + 3s)\mathbf{c}_{\text{av}}$
Transformation in reciprocal spaces	$\mathbf{a}^* = 4\mathbf{a}_{\text{av}}^* + r\mathbf{c}^*$ $\mathbf{b}_{\text{av}}^* = \mathbf{b}^*$ $\mathbf{c}^* = -3\mathbf{a}^* + (r + 3s)\mathbf{c}^*$	$\mathbf{a}^* = (9z - \frac{1}{2})\mathbf{a}_{\text{av}}^* + (12z - 1)\mathbf{c}_{\text{av}}^*$ $\mathbf{b}^* = \mathbf{b}_{\text{av}}^*$ $\mathbf{c}^* = \frac{1}{s}(21z - \frac{3}{2})\mathbf{a}_{\text{av}}^* + \frac{1}{s}(28z - 2)\mathbf{c}_{\text{av}}^*$

this modulation wavevector is shown in Fig. 6. The superspace group of this model is $X2/m(\alpha 0 \gamma)0s$ with the centering operation $X : (\frac{1}{2}, \frac{1}{2}, \frac{1}{2}, \frac{1}{2})$, $\alpha = (1/2 - 3z)$ and $\gamma = -4z$, equivalent to the superspace group number 12.2 in Janssen *et al.* (1992) or 12.1.4.2 in Stokes *et al.* (2011). Table 1 shows the symmetry elements of the superspace group and the possible space groups for the different t values of the three-dimensional section for any rational value of the m parameter, related to the composition. The known phases correspond to integer values of the m parameter, but analysis of the compatible three-dimensional space groups with a given superspace group can be extended to arbitrary rational compositions. The reason for representing some space groups in regular font and some others in bold format is as follows. The superspace model contains step-like (crenel) atomic domains where the occupation probability changes abruptly from 0 to 1. Then the atomic species are not as well defined at its borders. When the three-dimensional section crosses the limit of one of these step-like functions, the resulting three-dimensional structure becomes ambiguous and a full consistency with the assumed superspace symmetry would require the splitting of the occupational probability, hence modifying the initial structural model. These problematic sections, for specific t values, typically correspond to sections of high-symmetry. In Table 1 the t values not having this problem are indicated in bold. These are the three-dimensional symmetries that are fully compatible with the superspace model and are to be expected for commensurate values of the composition. This table is consistent with the reported space groups for $m = 4$ and $m = 5$ compounds. In the first case, $m = 4$ ($z = 3/40$), the reported (Pérez *et al.*, 1997) space group $P2_1/n$ corresponds to $t = 1/160$ and equivalent values of the t coordinate. In the second case, $m = 5$ ($z = 7/94$), the reported space group (Allix *et al.*, 2004) is $I2$, which corresponds to $t = 1/188$ and equivalent values of the t coordinate. Table 2 summarizes the relationship between the basis vectors of the average structure and of the superstructure for all compositions (including hypothetical non-integer values of m) both in direct and reciprocal spaces. Table 3 shows the structural parameters of

the atomic domains of the resulting ideal model, including the center ($x_1^0, x_2^0, x_3^0, x_4^0$) and width Δ of the atomic domains, the point group of the average positions and the restrictions on the displacive modulations due to the point symmetry.

There is a direct relationship between the internal space and the [307] direction of the three-dimensional structure, indicated by the dashed lines in Fig. 3. In this figure, consecutive metal atoms with $y \sim 0$ along the [307] direction (in the figure these are the metal atoms close to the nodes of the average lattice) are embedded into consecutive positions along the internal space in Figs. 6(a)–

(c). The same is true for the O atoms. It is also interesting to analyze the reciprocal space in the superspace approach. Fig. 7 shows a small region of the $(h0l)$ plane of the diffraction pattern of the $m = 5$ compound. In the figure both \mathbf{q}_w and \mathbf{q} modulation wavevectors have been included. It is clear that this compound cannot be considered a standard modulated structure, where the intensity of the satellite reflections is much smaller than the intensity of the main reflections and where the intensity decreases with the order of the satellite. As happens in other systems where there is a strong modulation in composition, there is not a clear hierarchy between the main reflections and satellite reflections of increasing order, but using the modulation wavevector of equation (5) the intense satellites are low-order satellites.

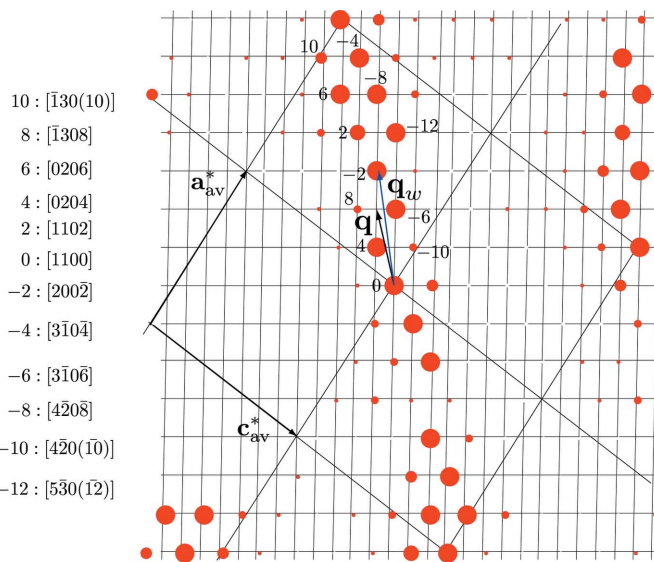


Figure 7
 Reproduction of a small part of Fig. 4. The blue arrow represents the *wrong* modulation wavevector \mathbf{q}_w given in equation (4) and the black arrow represents the modulation wavevector \mathbf{q} given in equation (5) and used to index the satellite reflections in the superspace approach of the $[\text{Bi}_4\text{Sr}_3\text{Fe}_2\text{O}_9]_m[\text{Bi}_4\text{Sr}_6\text{Fe}_2\text{O}_{16}]$ compound family.

Table 3

Superspace model for the $\text{Bi}_{4z}\text{Sr}_{6z}\text{Fe}_{1-10z}\text{O}_{4z+1}$ compound family: structural parameters.

Coordinates of the center of the atomic domains ($x_1^0, x_2^0, x_3^0, x_4^0$), width of the atomic domains, Δ , point symmetry of the center of the atomic domains and symmetry restrictions of the displacive modulations according to this point group. The Sr_x atom, represented by a continuous atomic domain, has been *artificially* included to make the refinement in a more efficient way using JANA2006 (Petříček *et al.*, 2006) – see text. The displacive modulations and the modulations of the displacement parameters of Fe, Sr and Bi atomic domains are restricted to the same values as for the atomic domain Sr_x. The general form of the displacive modulation for Sr_x includes even sine terms for the *x* and *z* components and odd sine terms for the *y* component. Parameters with asterisks are refinable. For O2, the following restriction has been applied: $t^0 = x_1^0 - \alpha x_1^0 - \gamma x_3^0 = \text{constant}$, where t^0 is the *t* coordinate of the center of the atomic domain and ($\alpha, 0, \gamma$) are the components of the modulation wavevector according to equation (5).

Structural parameters							
	x_1^0	x_2^0	x_3^0	x_4^0	Δ	Point symmetry	Modulation
Sr _x	0	0	0	0	–	2/ <i>m</i>	(sin(2),sin(1),sin(2))
Fe	0	0	0	0	$\frac{1}{2} - 5z$	–	Restricted
Sr	0	0	0	$\frac{1}{4}$	$3z$	–	Restricted
Bi	0	0	0	$\frac{1}{4} - 2z$	<i>z</i>	–	Restricted
O1	0	$\frac{1}{2}$ *	0	$\frac{1}{4}$	$5z$	2	(sin,cos,sin)
O2	$\frac{1}{4}$ *	$\frac{1}{4}$ *	$\frac{1}{4}$ *	0*	$\frac{1}{4} - \frac{3z}{2}$	1	General

4. Refinement of the (3 + 1)-dimensional model

Refinement within the superspace of the $m = 4$ and $m = 5$ compounds was started from the ideal model described in the previous subsection and given in Tables 1 and 3. The experimental data sets used in the refinements are the same data sets used in the original three-dimensional analysis for $m = 4$ (Pérez *et al.*, 1997) and $m = 5$ (Allix *et al.*, 2004) compounds. Technical information about the synthesis of the crystals and data collection can be found in these references. Some crystal data have been included in Table 4. The superspace unit cell contains five symmetry-independent atomic domains (see Table 3). However, the set of atomic domains representing the metal atoms with the same average position outline a continuous atomic domain along the internal space, as shown in Fig. 6. This is consistent with the fact that all the cells of the average lattice contain a metal atom close to the origin of the cell. Fig. 3 also shows that the relative displacements of the metal atoms with respect to their average position in the average unit cell vary smoothly from cell to cell along the dotted lines in the figures.

In the superspace construction of the structure this means that the displacive modulations to be included in the refined model will also be correlated, *i.e.* the set of atomic domains with the same average position will also follow a continuous and relatively smooth function along the internal space in this direction. Therefore, it is convenient to introduce some restrictions into the displacive functions that describe the modulations of the metal atoms. This can be done by forcing them to be described by the same functions. There is a simple way to introduce this restriction in the program used in the refinements, JANA2006 (Petříček *et al.*, 2006). It is possible to introduce an additional atomic domain in the model (named Sr_x in Table 3) with 0 occupation probability, so this atom does

Table 4

Some experimental and crystal data of the $m = 4$ ($z = 3/40$) and $m = 5$ ($z = 7/94$) members of the $\text{Bi}_{4z}\text{Sr}_{6z}\text{Fe}_{1-10z}\text{O}_{4z+1}$ 2212-type stair-like family as reported in the experimental original works (Pérez *et al.*, 1997; Allix *et al.*, 2004), unit-cell parameters of the average structure and components of the modulation wavevector in the $\{\mathbf{a}_{\text{av}}^*, \mathbf{b}_{\text{av}}^*, \mathbf{c}_{\text{av}}^*\}$ basis.

	$m = 4$	$m = 5$
<i>a</i> (Å)	16.491 (9)	16.553 (6)
<i>b</i> (Å)	5.481 (3)	5.495 (2)
<i>c</i> (Å)	30.086 (16)	35.305 (5)
β (°)	91.39 (2)	90.57 (8)
Space group	$P2_1/n$	$I2$
Index restrictions	$-26 \leq h \leq 26$ $0 \leq k \leq 8$ $0 \leq l \leq 46$	$-31 \leq h \leq 31$ $0 \leq k \leq 10$ $0 \leq l \leq 66$
Observed reflections ($I > 3\sigma$)	2671	6846
a_{av} (Å)	3.620 (2)	3.590 (2)
b_{av} (Å)	5.481 (3)	5.495 (2)
c_{av} (Å)	3.466 (2)	3.498 (2)
β_{av} (°)	81.25 (4)	81.92 (3)
q	$\frac{1}{40}(11, 0, -12)$	$\frac{1}{47}(13, 0, -14)$

not contribute to the scattering factor. This *ghost atom* is used as a mere intermediate to make possible the connection between neighbouring atomic domains along the internal space. The atomic domain of this artificial atom is located at the same average position as the independent metal atoms, and is continuous along internal space, as in a standard modulated structure. Then the coefficients associated with the displacive modulations and also the coefficients of the modulations of the thermal coefficients of the metal atoms are restricted to be the same as the coefficients of the Sr_x atom. In the structure refinement process we will then only refine the coefficients of the displacive modulations and thermal coefficients of this Sr_x atomic domain, thus reducing the number of independent atomic domains for the refinement from 5 to 3. Therefore, this single atomic domain describes the modulations of 20 (24) independent metal atoms in the real structure, 20 (23) in general positions and 0 (1) Sr atom on a twofold axis in the $m = 4$ (5) compound. The number of independent atoms described by a single atomic domain being so large we can expect that the number of Fourier components to be considered in the refinement will be high if we want to obtain a result comparable to the results obtained in the standard three-dimensional refinement. Due to the point symmetry of the Sr_x atomic domain, in the Fourier expansion series of the displacive modulations only even sine terms have to be included for the *x* and *z* components and only odd sine terms for the *y* component. The order of the last harmonic in the Fourier expansion series that can be considered in the refinement using JANA2006 for the Sr_x atomic domain is thus 40 (20 non-zero terms according to the point symmetry of the AD) for $m = 4$ and 47 (23 non-zero terms for *x* and *z* components and 24 for the *y* component) for $m = 5$. The dataset of the $m = 4$ and 5 phases includes observed reflections up to 20th and 46th order, respectively, so there is no problem introducing terms up to this order in the refinements. Using the maximum number of harmonics for the displacive modulations (and for the displacement parameters), the

Table 5

Results of the three-dimensional structure refinements and superspace refinements.

R factors are given for all reflections and, for four-dimensional refinements, also for the main ($n = 0$) and satellite reflections. Being a commensurate structure, the indexing (h, k, l, m) of the reflections is not unique. In all cases it has been assumed that the set of indices with the lowest $|m|$ is compatible with the superspace group. Observed reflections are those with $I > 3\sigma$. For the $m = 4$ phase, due to the small difference in the number of *observed* and *all* reflections, only the values of $R(\text{all})$ have been included.

Parameters	$m = 4$			$m = 5$		
	<i>N</i> ref. (obs)/all	4D ref. 131 <i>R</i> (all)	3D ref. 285 <i>R</i> (all)	<i>N</i> ref. (obs)/all	4D ref. 158 <i>R</i> (obs)/(all)	3D ref. 334 <i>R</i> (obs)/(all)
All	2671/2674	9.6	8.4	6846/11954	8.5/14.4	7.6/14.6
$n = 0$	104	9.3		187/257	7.3/9.0	
$n = 1$	81	5.8		289/443	6.4/11.2	
$n = 2$	206	10.4		390/509	7.9/9.7	
$n = 3$	76	7.1		265/448	6.3/12.3	
$n = 4$	181	9.1		368/510	8.9/10.9	
$n = 5$	80	5.8		274/436	5.8/10.9	
$n = 6$	185	10.9		369/509	8.1/11.2	
$n = 7$	70	8.4		270/447	7.6/13.1	
$n = 8$	248	10.0		377/502	7.8/10.1	
$n = 9$	67	8.1		246/437	8.6/14.8	
$n = 10$	206	9.1		375/509	7.1/9.3	
$n = 11$	63	7.9		237/438	9.1/17.7	
$n = 12$	230	8.6		380/508	7.2/10.5	
$n = 13$	52	8.2		216/442	10.9/19.6	
$n = 14$	244	10.1		324/516	7.9/13.2	
$n = 15$	42	9.0		239/441	11.7/20.1	
$n = 16$	196	11.3		308/507	7.6/13.7	
$n = 17$	33	9.2		205/444	12.2/22.4	
$n = 18$	198	10.7		251/507	9.6/18.4	
$n = 19$	28	11.5		196/440	12.0/23.4	
$n = 20$	84	14.8		227/510	11.9/22.4	
$n = 21$				211/445	11.9/23.5	
$n = 22$				244/503	11.8/21.7	
$n = 23$				171/438	13.8/27.7	
$n = 24$				25/68	12.3/30.9	
$n = 26$				34/64	15.4/25.0	
$n = 28$				23/70	18.7/32.5	
$n = 30$				22/68	18.7/32.5	
$n = 32$				21/66	22.5/38.0	
$n = 34$				15/70	21.2/47.1	
$n = 36$				13/65	31.2/56.1	
$n = 38$				14/69	23.9/54.2	
$n = 40$				20/64	26.0/39.4	
$n = 42$				13/69	15.1/54.3	
$n = 44$				8/66	34.5/48.4	
$n = 46$				19/69	26.7/48.0	
GoF(obs)/(all)		3.0	2.65		3.27/2.58	2.5/2.0

resulting model should be exactly the same as the three-dimensional model obtained in a standard refinement.

We start the refinement of the $m = 4$ compound introducing five non-zero terms (up to 10th harmonic) for each coordinate of the Sr_x atomic domain. In the first steps the O1 and O2 atoms are restricted to the average positions and the displacement parameters of all the atomic domains are fixed. This is a critical step in the refinement. The convergence is very slow and it is not guaranteed that the refinement process goes towards the absolute minimum. Sometimes the minimization process can be trapped in local minima. Finally, the R factor takes the $R = 27$ value for all and observed reflections. Afterwards, the number of Fourier terms were increased up to $n = 30$ for Sr_x (15 non-zero terms for each coordinate), reducing the R factor to $R = 14.8$ for all and observed

reflections. Next, the parameters defining the O1 and O2 atoms were taken into consideration. First, the average positions and then the displacive modulations were introduced in the refinement. The widths of the atomic domains are $\Delta = 0.375$ and 0.1375 for O1 and O2, respectively. Therefore, the standard harmonic functions used in the Fourier series are not orthogonal in the restricted interval of the internal space where the atomic domains are defined. Several solutions have been proposed to keep the orthogonality of the functions. A widely used set of functions in the superspace analysis of compounds that contain small atomic domains is the so-called *ortho* functions (Petříček *et al.*, 1995), obtained through a Schmidt orthogonalization routine. However, using this set of functions for O1 and O2 atomic domains, the refinements hardly converged and the final results included huge values of the amplitudes associated with the *ortho* functions. The displacive modulations showed a wavy behavior with large displacements with respect to the average position and long tails at the borders of the atomic domains. When this happens, it is possible to have acceptable atomic positions when the three-dimensional section is considered, but it is necessary to include the maximum number of functions and their large amplitudes correlate in such a way that they give the correct values at the specific relevant t points of the functions describing the atomic positions in real space. These functions are normally strongly dependent on this set of t points. For other compositions, with a different number

of relevant t values, it will also be necessary to consider the maximum number of terms in the function series, their amplitudes will also correlate (but in a different way, in general) to give the correct values at the specific t values of the function. A specific *ad hoc* set of displacive modulations is thus required for each compound and therefore their approximate form is not transportable from one compound to another. With this parameterization, the use of the superspace formalism would lose a good part of its advantage for these atomic domains.

Therefore, we decided to use the Legendre polynomials introduced in *JANA2006* in 2008 as base functions to describe an arbitrary displacive modulation (Dušek *et al.*, 2010). Two Legendre polynomials for O1 and a single polynomial for O2 were initially introduced, and the refinement converged very

fast, reducing the R parameter to $R = 13.8$. In the final steps the number of functions used to reproduce the displacive modulations of all the independent atomic domains and the modulations of the displacement parameters were increased until reasonable R parameters were obtained. Table 5 shows the final results of the refinement and they are compared with the results obtained by a three-dimensional refinement. More detailed information about the refinement can be obtained in the supplementary material.¹ Up to 18 terms have been necessary for each component of the displacive modulation and seven for the modulation of the thermal coefficients of the Sr_x atomic domain. For O1 and O2 atomic domains, only four non-zero amplitudes of the low-order Legendre polynomials have been considered. No modulations of the isotropic displacement coefficients were necessary for these two atomic domains. The final number of parameters (131) represents a reduction of 54% with respect to the number of parameters (285) needed in the standard three-dimensional refinement. The difference in the R values obtained in the four-dimensional and three-dimensional analyses is 1.3 ($R = 9.64$ in the four-dimensional refinement against $R = 8.35$ in three-dimensional refinement). The large number of Fourier terms used to represent the Sr_x atomic domain is justified considering the large number (20) of independent metal atoms that this atomic domain represents and the existence of very high-order satellite reflections within the indexing scheme used. In fact, for the positional parameters the advantage of the use of the superspace model is slight (18 parameters instead of 20), as it was necessary to reach nearly the maximum number of parameters. The largest difference in the number of parameters originates in the small number of modulation functions used for the ADP of the Sr_x atomic domain. The refined atomic domains are sketched in Fig. 8. The commensurate points within the atomic domains describing the real space atomic positions are also shown. Different colors (black, white, gray) have been used to indicate the atomic domains representing the three different cations, Sr, Bi and Fe. To be noted are the large scale of the displacive modulations along the x and z directions (in the defined average cell), with displacements with respect to the average position of the order of 1 Å. The continuity of the modulations between consecutive atomic domains along the internal space, corresponding to different cations, is also remarkable. In other families of compounds the cation substitution introduces important local rearrangements that are reflected in strong modulation discontinuities when passing from one metal atom domain to another along the internal space. In the present systems, however, this effect is weak, especially for the interfaces between the Fe and Sr domains. It could be argued that this feature has been forced in the refined model, as the modulations of the metal atom domains have been described by a single continuous function associated with the virtual atom Sr_x. However, it should be taken into account that the

number of Fourier terms used in the refinement is close to the complete set, so that, in practice, each of the commensurate points in the domains was essentially free in the refinement.

The figures also allow us to analyze the differences between the superspace models using the *wrong* and *good* modulation wavevectors given by equations (4) and (5), respectively. The x_1 and x_3 components of the displacive modulation have 1/2 subperiodicity. Only even sin terms are included in the Fourier expansion series (see Table 6 of the supplementary material). The subperiodicity is only broken by the x_2 component of the modulation. Using the modulation vector given by equation (4) instead of equation (5), there would be no modulation of the x_2 component and, therefore, it would be an exact subperiodicity of 1/2 along the internal space, and the atomic domain distribution shown in Fig. 5 would be recovered. In that case, the resulting space groups would be $B2/m$ for $m = 4$ and $I2/m$ for $m = 5$, according to the discussion in §3.2.

Finally, it is interesting to point out that the largest amplitude is associated with the non-zero second term in the

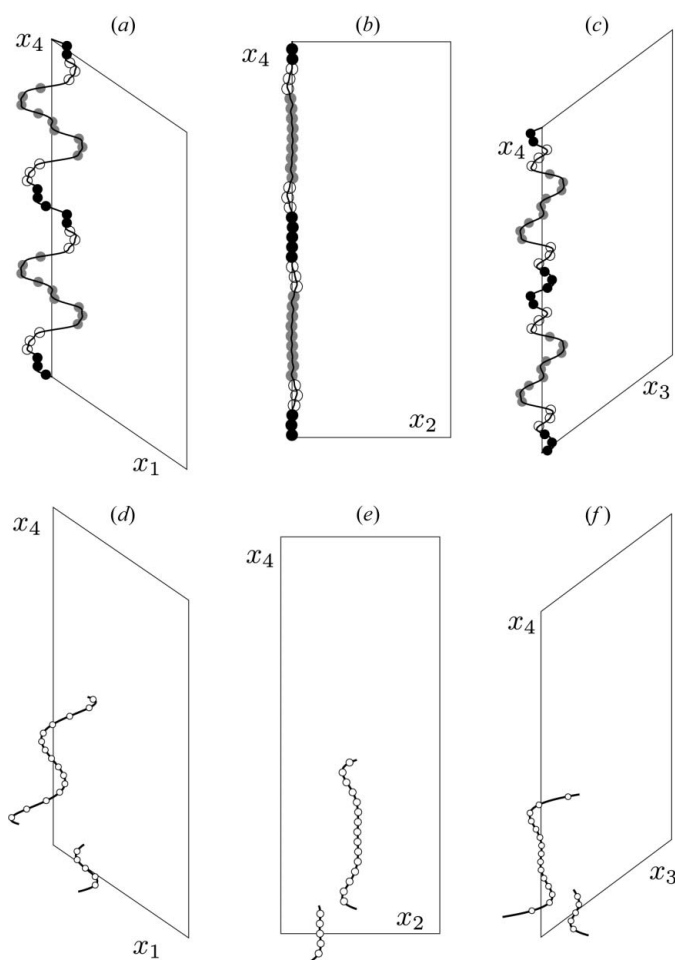


Figure 8 Projections (a) (x_1, x_4) , (b) (x_2, x_4) and (c) (x_3, x_4) of the refined Sr_x atomic domain and points representing Fe (black), Bi (white circle) and Sr (gray) atoms in the Sr_x atomic domain. Projections (d) (x_1, x_4) , (e) (x_2, x_4) and (f) (x_3, x_4) of the refined atomic domains O1 and O2 (see Table 3). The refined parameters of the displacive modulations are given in Table 6 of the supplementary material. Color labels are as in Fig. 2.

¹ Supplementary data for this paper are available from the IUCr electronic archives (Reference: BP5040). Services for accessing these data are described at the back of the journal.

Fourier expansion series of the displacive modulation of the Sr_x atomic domain (fourth-order harmonic), as can be seen in Fig. 9 and in Table 6 of the supplementary material. Thus it seems that there are two competing primary modulation wavevectors, \mathbf{q} for the occupation modulation and $4\mathbf{q}$ for the displacive modulation. As the structure is commensurate, it would be possible in the analysis to assume $4\mathbf{q}$ as the primary modulation wavevector rather than \mathbf{q} . All the reflections could also be indexed under the new basis, but the points representing the atomic positions in the Sr_x atomic domain would be rearranged, and the crenel-like atomic domains would be divided into smaller pieces increasing the number of independent atomic domains. Therefore, it is not advisable to take this alternative vector as the primary modulation wavevector.

The next step was to refine the structure of the other compound ($m = 5$) with a known structure and the available diffraction data. It was possible to start the refinement from the ideal model given in Tables 1 and 3 and outlined in Fig. 6, as has been carried out for the $m = 4$ phase. However, once a common superspace model for the compound series was defined, a fundamental point to be checked was the *transportability* between different compounds of the displacive modulations to be added to the common reference model described in terms of crenels. Thus, we started the refinement of the $m = 5$ compound taking the refined model of the $m = 4$ compound as the starting point, fixing the displacive modulations and the (modulated) displacement parameters and refining only the scale. It is necessary to just change the widths of the atomic domains and the x_4^0 component of the center of the Bi atomic domain according to Table 3, and slightly modify the cell parameters of the average structure (see Table 4). We are thus assuming that the functional form of the displacive functions is the same, despite being defined in a different range of values of t or x_4 . The R factor for this starting model with only the scale factor refined was $R = 0.145$ for the observed reflections. This value indicates that the refined model of the $m = 4$ member of the family is a very good approximation of the structure of the next member $m = 5$. In fact, it is very close to the final model. It can be stated that the correlations between the atomic positions described by the modulation functions are almost the same in both compounds, such that the displacive modulations, despite the different compositions and size of the supercells, are approximately invariant. To finish the structure refinement of the $m = 5$ compound, the starting values of the displacive modulations and the displacement parameters were refined and more terms were included in several steps. The final results of the refinement are included in Table 5. The amplitudes associated with the expansion series of the atomic domains (harmonic functions for Sr_x and Legendre polynomials for O1 and O2) are given in Table 6 of the supplementary material.

Figs. 9 and 10 show the superposition of the displacive modulations present in the two phases investigated, $m = 4, 5$, with respect to the idealized common superspace model. The relevant points of the atomic domains, *i.e.* those points in the atomic domain that give an atomic position when the three-dimensional section is considered, have also been included in

the figures. A most striking feature of the modulations is the impressive similarity in this scale of the displacive modulations for all the components and for all the independent atoms in both phases. The similarity is even more remarkable if we take into account that the Sr_x atomic domain is divided into regions representing atoms of different species (and whose relative sizes are different for different compositions), and that the number of Fourier terms used is unusually high. It can be said undoubtedly that there is a unique model in the superspace for these two compounds, which includes the displacive modulations. Of course, the modulation functions are not exactly the same in both compounds, and there are some slight deviations, in particular in the oxygen domains. However, the degree of coincidence of the modulations in the scale of the figures is

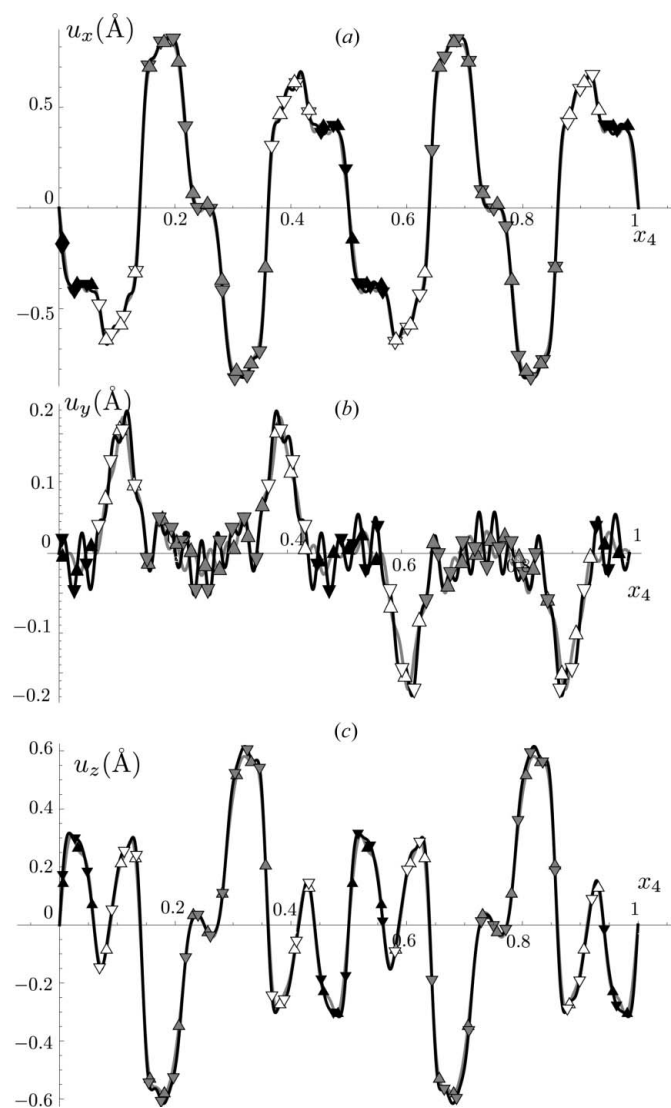


Figure 9
 x_4 dependence of the (a) x , (b) y and (c) z component of the displacive modulation (in Å) of the Sr_x atomic domain for $m = 4$ (gray curve) and $m = 5$ (black curve). The relevant points that give an atomic position when the three-dimensional section is considered are also shown for $m = 4$ (up triangles) and $m = 5$ (down triangles). There is an extraordinary similarity between the modulations of both phases. Color labels for the metal atoms are as in Fig. 2.

remarkable, and demonstrates that the two structures possess strong correlations beyond the three-dimensional space group that can be described by these modulations which are common for the two compounds. These figures also permit analysis of the correlations between the displacements of the atoms inside the [BiO], [SrO] or [FeO₂] columns (units) and also the correlations between neighbouring units in the [BiO]_{*m*+2}, [SrO]_{3(*m*+2)} and [FeO₂]_{2*m*+2} blocks. Fig. 9(b) shows that the Sr and Fe atoms remain, basically, in the *y* = 0 layer, having the Bi atoms the largest out of layer displacements among the metal atoms (~ 0.15 Å). Comparing Figs. 8(b) and (e) we see that the modulations of the O and Bi atoms in the [BiO] units

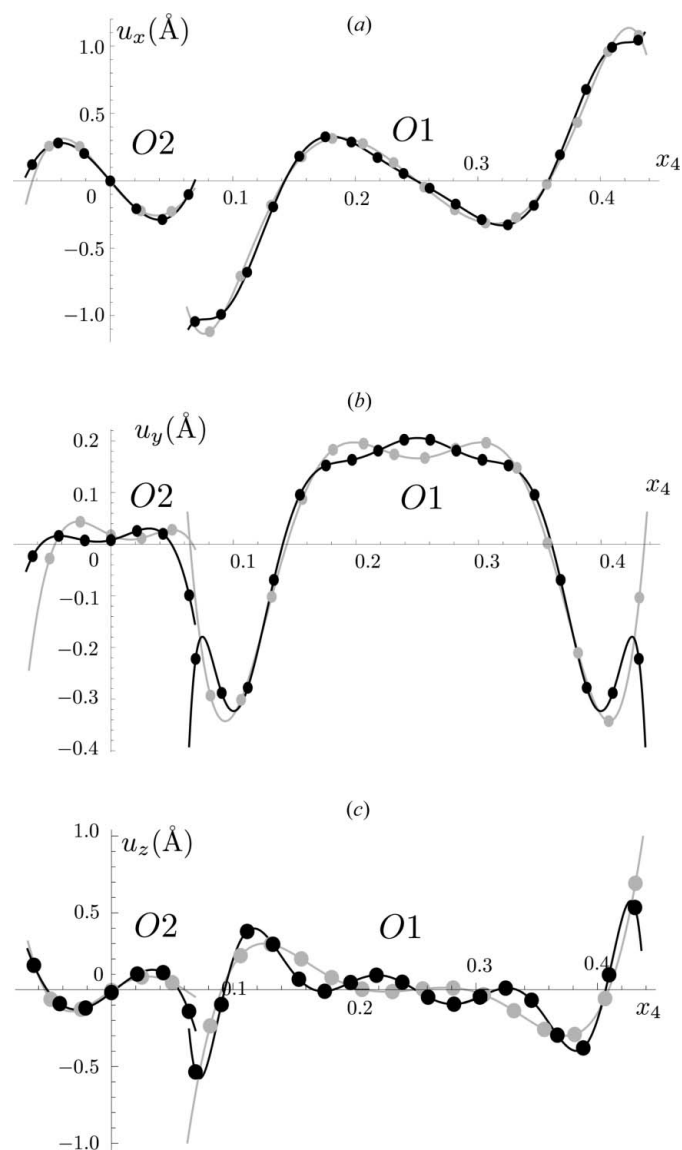


Figure 10
 x_4 dependence of the (a) *x*, (b) *y* and (c) *z* component of the displacive modulation (in Å) of the O1 and O2 atomic domains for *m* = 4 (gray curve) and *m* = 5 (black curve). The relevant points that give an atomic position when the three-dimensional section is considered are also shown. There is an extraordinary similarity between the modulations of both phases.

are correlated in such a way that the [BiO] columns can be considered, to a first approximation, as rigid units. Also taking into account the atomic domains shifted $(\frac{1}{2}, \frac{1}{2}, \frac{1}{2})$ with respect to the independent atomic domains in the figures, it can be seen that neighbouring [BiO] units are shifted in-phase in the (*x*, *z*) plane and out-of-phase along the *y* direction in the [BiO]_{*m*+2} blocks. Inside a [SrO] column, the O atom approaches one of the neighbouring metal atoms and, inside a [SrO]_{3(*m*+2)} block, the displacements of the O atoms in neighbouring units are out of phase.

The results of the refinements indicate that the displacive modulations are basically invariant and do not depend on a member of the family. We can therefore assume the uniqueness of the superspace model for at least some range of the composition and propose realistic three-dimensional structure models for other members of the family. We can consider the previous member (*m* = 3), the subsequent one (*m* = 6) and also a hypothetical intergrowth compound of the two known phases, *m* = 9/2. According to the general stoichiometric formula, the compositions of these three compounds are Bi₁₀Sr₁₅Fe₈O₄₃ for *m* = 3 (*z* = 5/66), Bi₈Sr₁₂Fe₇O₃₅ for *m* = 6 (*z* = 2/27) and Bi₂₆Sr₃₉Fe₂₂O₁₁₃ for *m* = 9/2 (*z* = 13/174). If we assume the allowed space groups of higher symmetry as given in Table 1, they should be *I*2 for *m* = 3, *P*2₁/*n* for *m* = 6 and *P*2/*a* for *m* = 9/2. The cell parameters of the resulting superstructures can be calculated from Table 2. Next, we substitute the value of the composition parameter *z* into the x_4^0 component of the center of the Bi atomic domain and into the expression of the widths of all the atomic domains in Table 3. Finally, taking the same parameters as those describing the displacive modulations given in Table 6 of the supplementary material for *m* = 5, we obtain the structures shown in Fig. 11. The atomic distribution of the hypothetical *m* = 3 and *m* = 6 members of the 2212-type stair-like phases can be helpful for simulations of HREM images but also are a very good starting point for their structure refinement (using powder diffraction for instance).

5. Conclusions

The results presented here show that a unique superspace model exists to describe the known members of the stair-like family of compounds related to the Bi-2212 phase. A single superspace group, single average structure and composition-dependent modulation wavevector underlies both structures. The superspace group proposed yields the different three-dimensional space groups reported for the two structures. Interest in such (3 + 1)-dimensional analysis has been demonstrated for a long time. A global understanding of the symmetry of the family *versus* the composition as well as a reduction in the number of refinement parameters is expected. The superspace approach usually makes evident the correlation between the structure parameters of different compounds of the same family. Then such a description also provides a useful tool to predict the structures of new members. However, in the present study the superspace analysis even goes beyond these usual expectations. The present model also

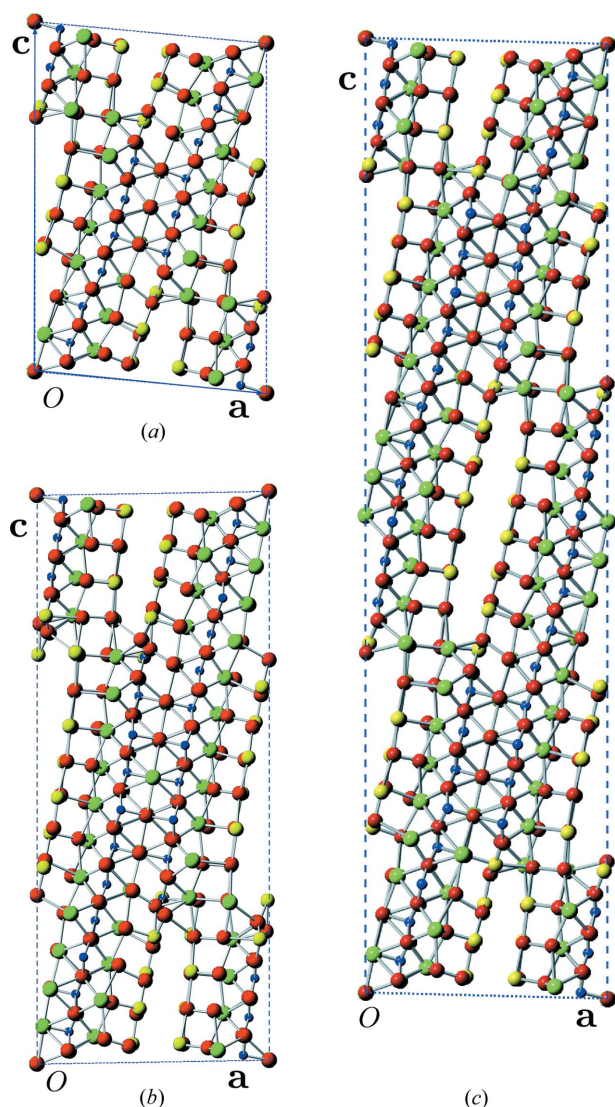


Figure 11
 Predicted structures for the (a) $m = 3$, (b) $m = 6$ and (c) $m = 9/2$ members of the family of compounds assuming as displacive modulation functions the refined ones for the $m = 5$ member. Color labels are as in Fig. 1. This figure is in colour in the electronic version of this paper.

shows that the more subtle details of the structures as the relative displacements of the atoms with respect to the idealized average structure, parametrized in the superspace as displacive modulations, are basically the same in the 2212 terrace-like family. These displacive modulation seems to be independent of the compound: a unique model allows the description of the entire 2212 stair-like structure!

Furthermore, shearing mechanisms are relatively frequently observed in the Bi–Sr–Ca– M –O systems (with $M = \text{Fe}, \text{Cu}, \text{Mn}$ or Co). Very often, stair-like arrangements are observed but only on short-range domains. Structural analyses are not possible in these cases. The interpretation and then the simulation of the HREM images require an accurate structural model such as those defined in this article. Moreover, recent investigations on the Sr–Fe–O system show the possibility of

generating 2201 and 2212 modulated phases based on the building of double infinite layers $[\text{FeO}]_{\infty}$ – $[\text{FeO}]_{\infty}$ rather than $[\text{BiO}]_{\infty}$ – $[\text{BiO}]_{\infty}$ (Perez *et al.*, 2006; Grebille *et al.*, 2006). In these new systems, stair-like structures have been reported (Lepoittevin *et al.*, 2006). The generalization of the (3 + 1)-dimensional model determined for the $[\text{Bi}_2\text{Sr}_3\text{Fe}_2\text{O}_9]_m$ – $[\text{Bi}_4\text{Sr}_6\text{Fe}_2\text{O}_{16}]$ series for these new systems could be of great interest for developing this field of material chemistry.

From a more technical point of view, this study reveals that the Legendre polynomials are a very good option to reproduce the complex displacive modulations defined on a crenel-like atomic domain of small size.

This work has been supported by the Basque Government (Project No. IT-282-07), the Spanish Ministry of Science and Innovation (Project MAT2008-05839), the SPRI (Project S-PE11UN040) and developing of the JANA2006 program is supported by Praemium Academiae of the Czech Academy of Sciences.

References

- Allix, M., Pérez, O., Pelloquin, D., Hervieu, M. & Raveau, B. (2004). *J. Solid State Chem.* **177**, 3187–3196.
- Darriet, J., Elcoro, L., Abed, A. E. & Perez-Mato, J. M. (2002). *Chem. Mater.* **14**, 3349–3363.
- Darriet, J., Weill, F., Darriet, B., Zhang, X. F. & Etorneau, J. (1993). *Solid State Commun.* **86**, 227–230.
- Dušek, M., Petricek, V. & Palatinus, L. (2010). *J. Phys.* **226**, 012014.
- Elcoro, L., Perez-Mato, J. M., Friese, K., Petříček, V., Balić-Zunić, T. & Olsen, L. A. (2008). *Acta Cryst.* **B64**, 684–701.
- Elcoro, L., Perez-Mato, J. M. & Withers, R. (2000). *Z. Kristallogr.* **215**, 727–739.
- Elcoro, L., Zúñiga, F. J. & Perez-Mato, J. M. (2004). *Acta Cryst.* **B60**, 21–31.
- Grebille, D., Lepoittevin, C., Malo, S., Perez, O., Nguyen, N. & Hervieu, M. (2006). *J. Solid State Chem.* **179**, 3849–3859.
- Hervieu, M., Caldes, M. T., Cabrera, S., Michel, C., Pelloquin, D. & Raveau, B. (1995a). *J. Solid State Chem.* **119**, 169–175.
- Hervieu, M., Caldes, M. T., Cabrera, S., Michel, C., Pelloquin, D. & Raveau, B. (1995b). *J. Solid State Chem.* **118**, 357–366.
- Hervieu, M., Michel, C., Caldes, M. T., Pham, A. & Raveau, B. (1993). *J. Solid State Chem.* **107**, 117–126.
- Hervieu, M., Michel, C., Nguyen, N., Retoux, R. & Raveau, B. (1988). *Eur. J. Solid State Inorg. Chem.* **25**, 375.
- Hervieu, M., Michel, C., Pham, A. & Raveau, B. (1993). *J. Solid State Chem.* **104**, 289–301.
- Hervieu, M., Pérez, O., Groult, D., Grebille, D., Leligny, H. & Raveau, B. (1997). *J. Solid State Chem.* **129**, 214–222.
- Izaola, Z., González, S., Elcoro, L., Perez-Mato, J. M., Madariaga, G. & García, A. (2007). *Acta Cryst.* **B63**, 693–702.
- Janner, A. & Janssen, T. (1980a). *Acta Cryst.* **A36**, 399–408.
- Janner, A. & Janssen, T. (1980b). *Acta Cryst.* **A36**, 408–415.
- Janssen, T., Chapuis, G. & de Boissieu, M. (2007). *From Modulated Phases to Quasicrystals*. Oxford University Press.
- Janssen, T., Janner, A., Looijenga-Vos, A. & de Wolf, P. M. (1992). *International Tables for Crystallography*, edited by A. J. C.

- Wilson, Vol. C, pp. 797–835. Dordrecht: Kluwer Academic Publishers.
- Lepoittevin, C., Malo, S., Perez, O., Nguyen, N., Maignan, A. & Hervieu, M. (2006). *Solid State Sci.* **8**, 1294–1301.
- Michiue, Y., Yamamoto, A. & Tanaka, M. (2006). *Acta Cryst.* **B62**, 737–744.
- Pérez, O., Elcoro, L., Perez-Mato, J. M. & Petříček, V. (2012). To be submitted.
- Pérez, O., Leligny, H., Baldinozzi, G., Grebille, D., Hervieu, M., Labbé, P., Groult, D. & Graafsma, H. (1997). *Phys. Rev. B*, **56**, 5662–5672.
- Perez, O., Mellenne, B., Retoux, R., Raveau, B. & Hervieu, M. (2006). *Solid State Sci.* **8**, 431–443.
- Perez-Mato, J. M., Elcoro, L., Aroyo, M. I., Katzke, H., Tolédano, P. & Izaola, Z. (2006). *Phys. Rev. Lett.* **97**, 115501.
- Perez-Mato, J. M., Elcoro, L., Petříček, V., Katzke, H. & Blaha, P. (2007). *Phys. Rev. Lett.* **99**, 025502.
- Perez-Mato, J. M., Zakhour-Nakhl, M., Weill, F. & Darriet, J. (1999). *J. Mater. Chem.* **9**, 2795–2808.
- Petříček, V., Dusek, M. & Palatinus, L. (2006). *JANA2006*. Institute of Physics, Praha, Czech Republic.
- Petříček, V., van der Lee, A. & Evain, M. (1995). *Acta Cryst.* **A51**, 529–535.
- Schmid, S., Fütterer, K. & Thompson, J. G. (1996). *Acta Cryst.* **B52**, 223–231.
- Schmid, S. & Withers, R. (1994). *J. Solid State Chem.* **109**, 391–400.
- Stokes, H. T., Campbell, B. J. & van Smaalen, S. (2011). *Acta Cryst.* **A67**, 45–55.
- Thompson, J., Withers, R., Sellar, J., Barlow, P. J. & Hyde, B. G. (1990). *J. Solid State Chem.* **88**, 465–475.
- van Smaalen, S. (2007). *Incommensurate Crystallography*. Oxford University Press.
- Wolff, P. M. de (1974). *Acta Cryst.* **A30**, 777–785.